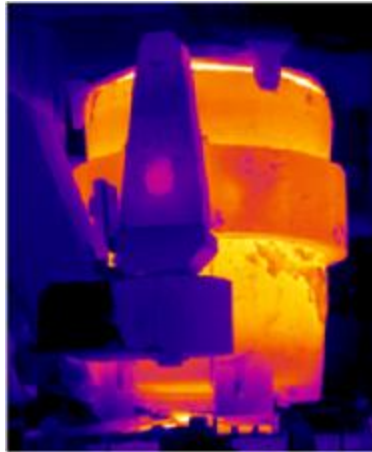


# Present Status of Thermomechanical Lining Simulation

Shengli Jin, Harald Harmuth, Dietmar Gruber

Feuerfest-Symposium 2018, Freiberg



## Service conditions of refractories

- High temperature
- Hot thermal shock
- Cold thermal shock
- Cyclic operation
- Mechanical constraints

.....



## A fact

The thermomechanical **wear process** cannot be **observed directly** in service or easily identified after service!

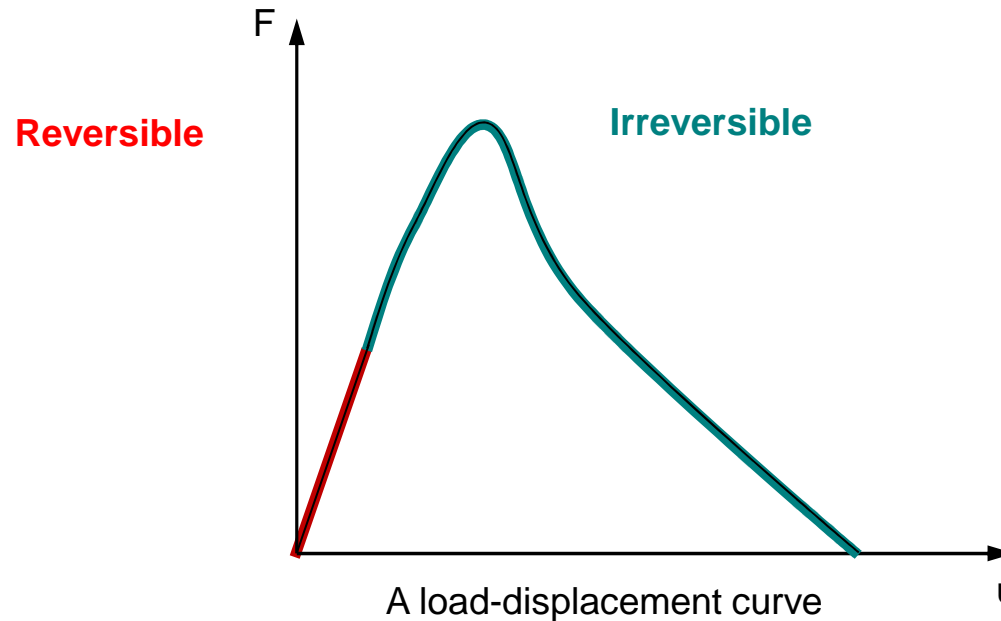
## Finite element method

- is a useful tool to **visualize** the performance of refractory linings under complicated process conditions
- brings about an understanding of the **thermomechanical wear mechanisms** of industrial vessels and gives rise to **an extended campaign life**

## The following knowledge will increase the understanding of advanced finite element thermomechanical modelling

- **Types of refractory behavior**
- Reasonable applications of **material constitutive models**
- Corresponding **characterization measures** for refractories at various temperatures

## Refractory behavior



### Defining reversible behavior

Young's modulus  $E$

Shear modulus  $G$

Poisson's ratio  $\nu$

Coefficient of thermal expansion  $\alpha$

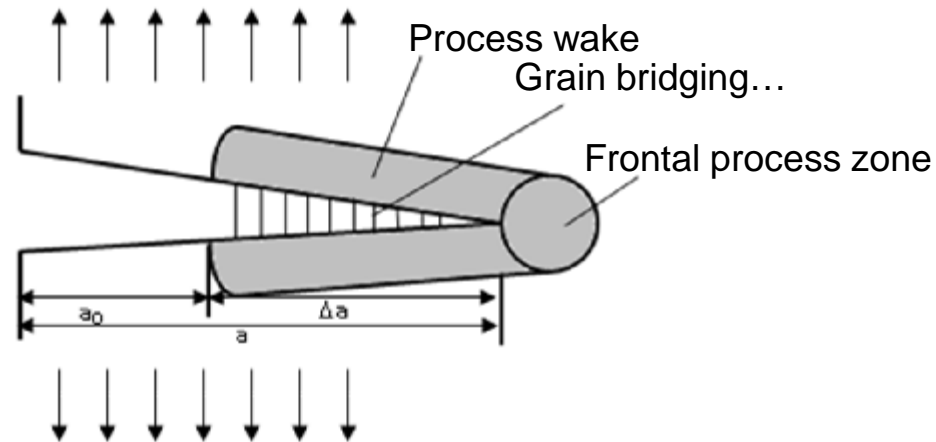
### Causes of irreversible behavior

Tensile failure

Shear failure

Creep or/and shrinkage

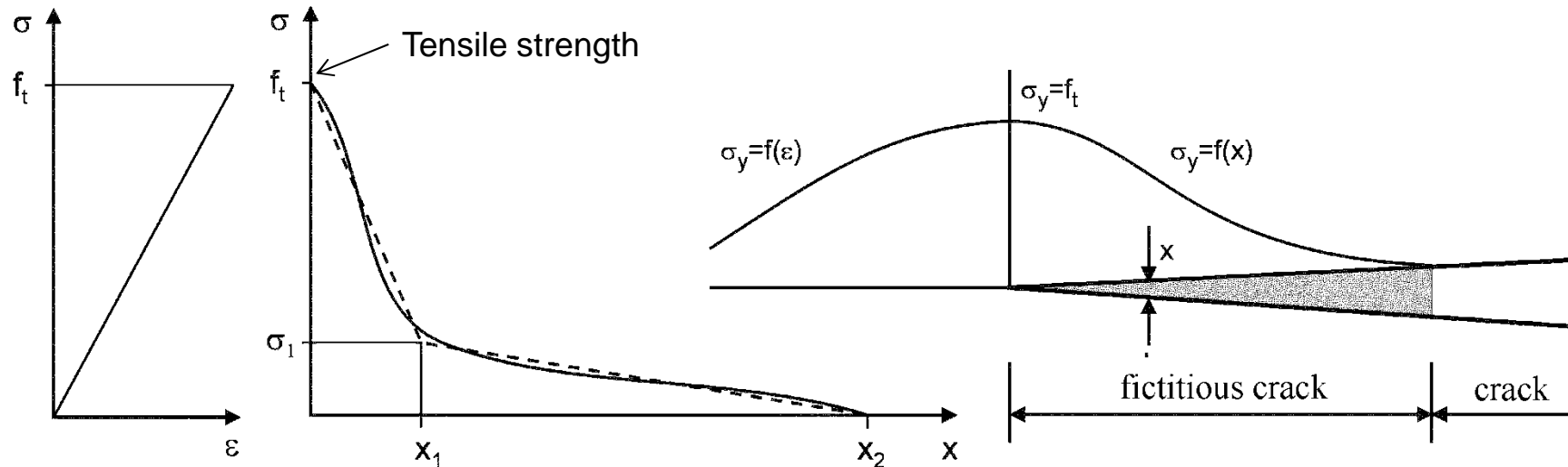
## Material constitutive model accounting for tensile failure



### Deviations from pure linear elastic fracture mechanics

- Linear stress/strain laws may be applied as a reasonable approximation for refractory behaviour as long as failure does not occur
- In cases of failure usually irreversible displacement remains
- Fracture energy is dissipated within a process zone
- Due to a process zone, the definition and measurement of a crack length is not possible

## Material constitutive model accounting for tensile failure



*Fictitious crack model proposed by Hillerborg*

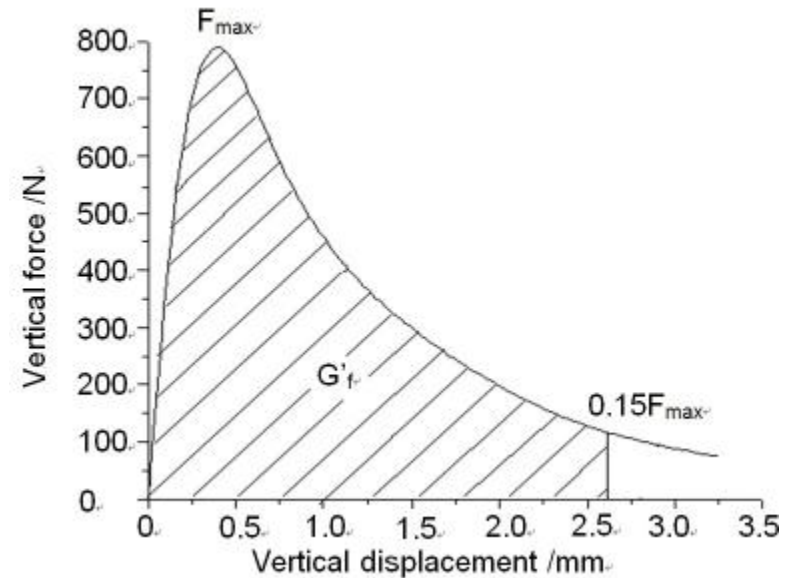
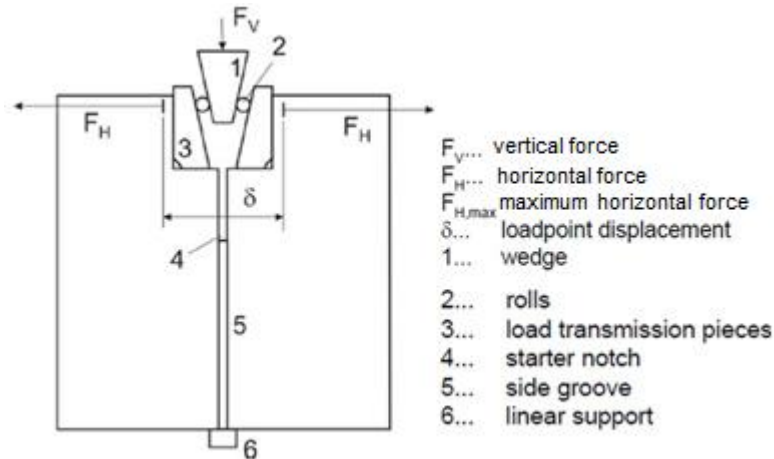
Fracture energy 
$$G_f = \int_0^{x_2} \sigma(x) dx$$

Characteristic length 
$$l_{ch} = \frac{G_f E}{f_t^2}$$

$l_{ch}$  is proportional to  $R''''$  (thermal shock damage resistance parameter)

## Characterization method for tensile failure

### Wedge splitting test



$$F_H = \frac{F_V}{2 \tan \frac{\alpha}{2}}$$

$$G_f = \frac{1}{A} \int_0^{d_{max}} F_H dd$$

$$s_{NT} = \frac{F_{H,max}}{bh} \frac{y}{e} + \frac{6y}{h} \frac{\delta}{\phi}$$

$\alpha$ : Wedge angle

$A$ : Fracture surface area

$y$ : The vertical distance of the center of gravity of the fracture surface from the horizontal force

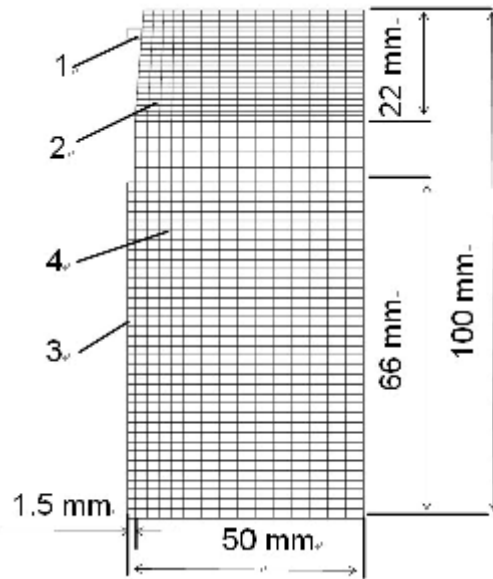
$h$ : Height

$b$ : Width

$G'_f < G_f$  due to termination of test at relatively low loads

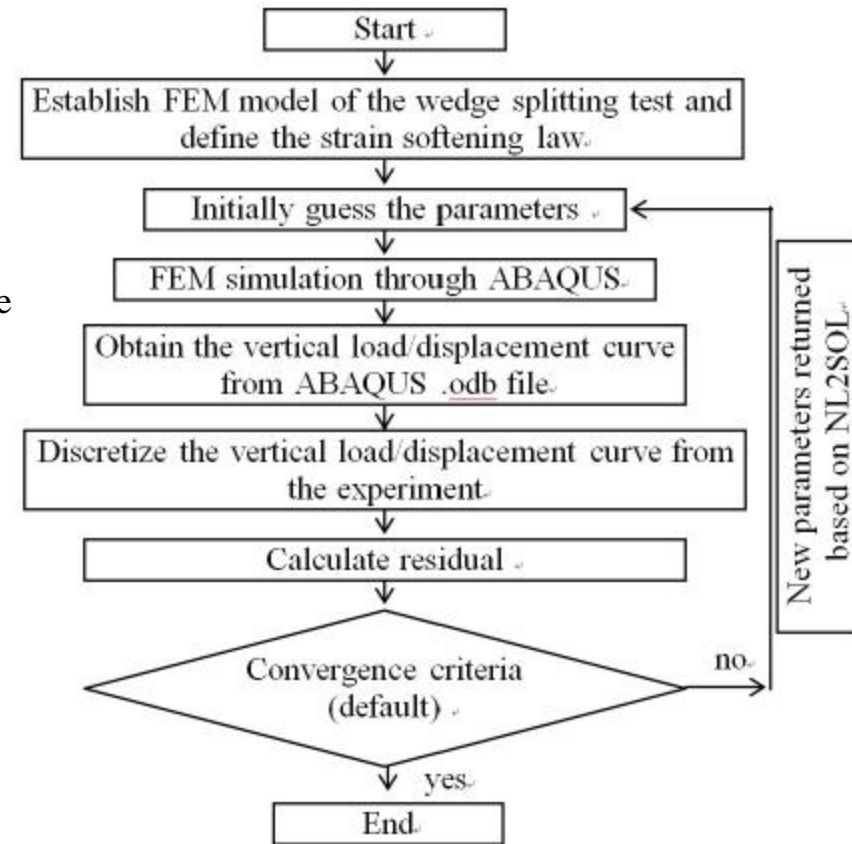
$G_f$   $f_t$  are anonymous

## Characterization method for tensile failure



- 1-roller,
- 2-load transmission piece
- 3-ligament area,
- 4-linear elastic part of specimen

Two-dimensional and symmetrical model for the wedge splitting test

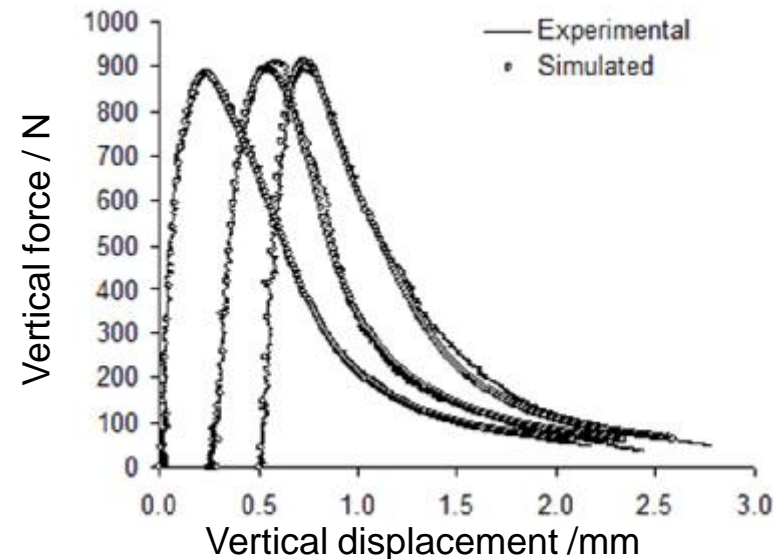


the flowchart of inverse estimation process

S. Jin, D. Gruber, H. Harmuth. Determination of Young's modulus, fracture energy and tensile strength of refractories by inverse estimation of a wedge splitting procedure. Engineering Fracture Mechanics, 2014, 116: 228-236.



## Characterization method for tensile failure



Experimentally and simulated curves of a burnt magnesia-chromite material at room temperature

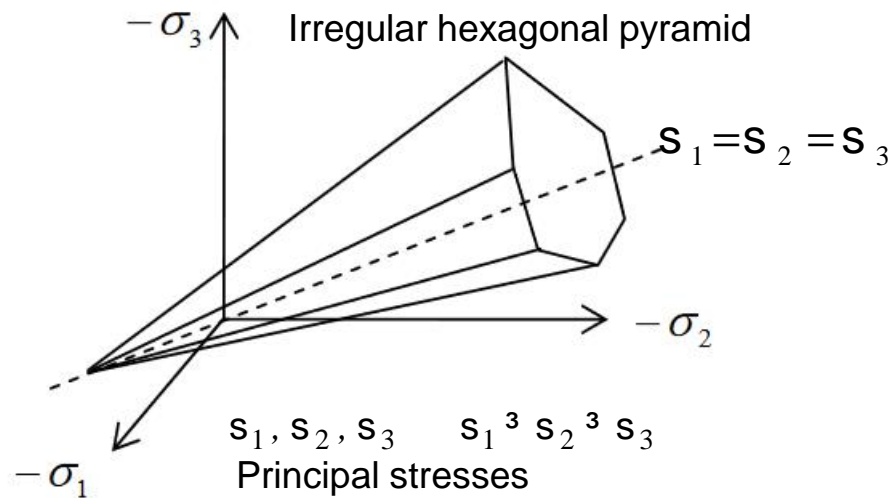
Experimentally obtained and inversely estimated parameters of a burnt magnesia-chromite material at room temperature

	Experiment	Inverse estimation
Fracture energy, / $\text{N}\cdot\text{m}^{-1}$	151	177
Strength, / MPa	8.9	5.5
$l_{ch}$ / mm	156	475

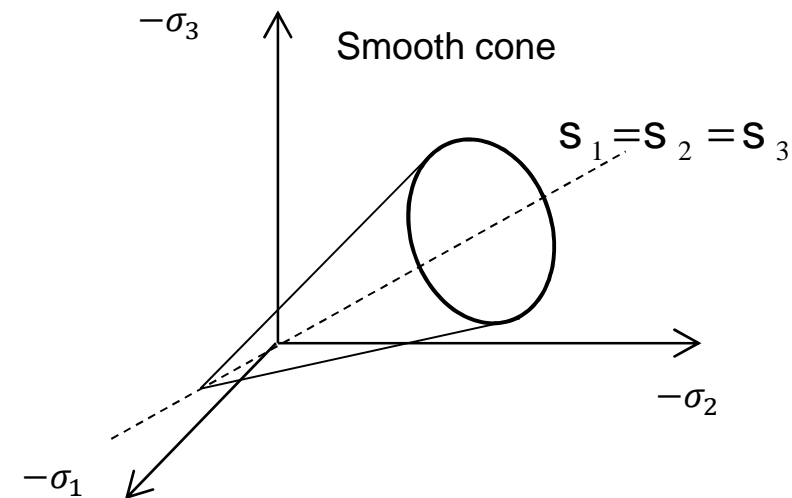
S. Jin, D. Gruber, H. Harmuth. Determination of Young's modulus, fracture energy and tensile strength of refractories by inverse estimation of a wedge splitting procedure. Engineering Fracture Mechanics, 2014, 116: 228-236.

## Material constitutive model accounting for shear failure

The capacity of geomaterials to resist shear failure is pressure dependent



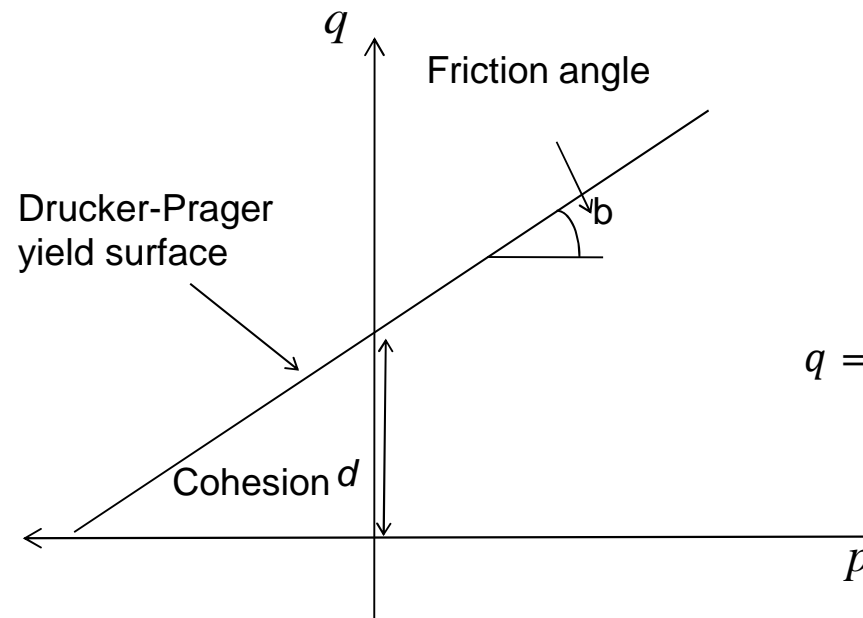
Mohr-Coulomb yield surface in principal stress coordinates



Drucker-Prager yield surface in principal stress coordinates

- The **Mohr-Coulomb criterion** does **not account** the contribution of **the intermediate principal stress** and disagreements with experimental results are often discovered
- The **Drucker-Prager criterion** is **preferable**

## Material constitutive model accounting for shear failure



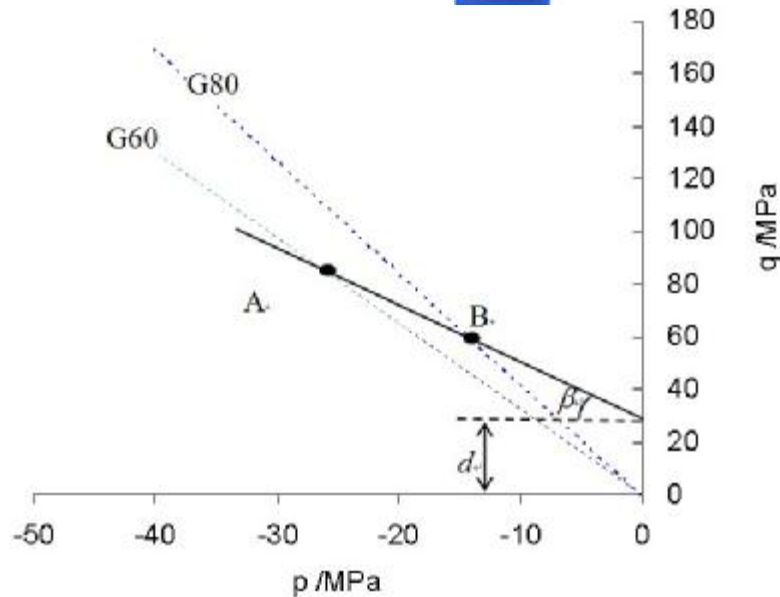
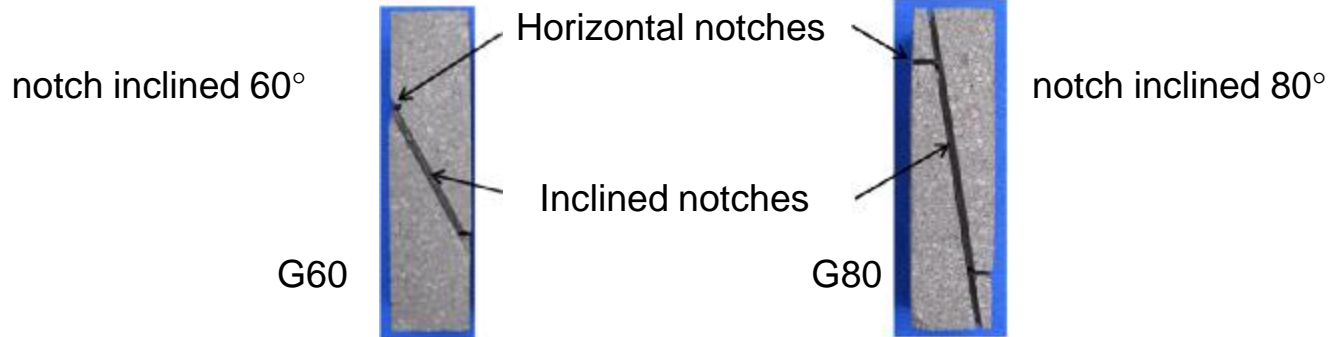
$$p = \frac{\sigma_1 + \sigma_2 + \sigma_3}{3}$$

$$q = \sqrt{\frac{1}{2}((\sigma_1 - \sigma_2)^2 + (\sigma_2 - \sigma_3)^2 + (\sigma_1 - \sigma_3)^2)}$$

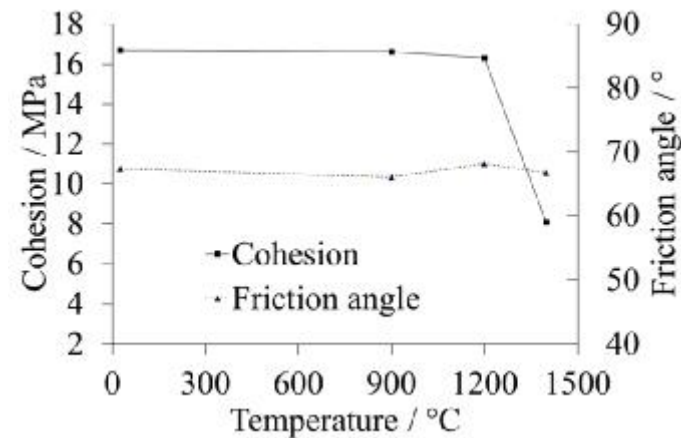
Drucker-Prager model in p-q diagram

- Determination of friction angle and cohesion is necessary

### Characterization method for shear failure



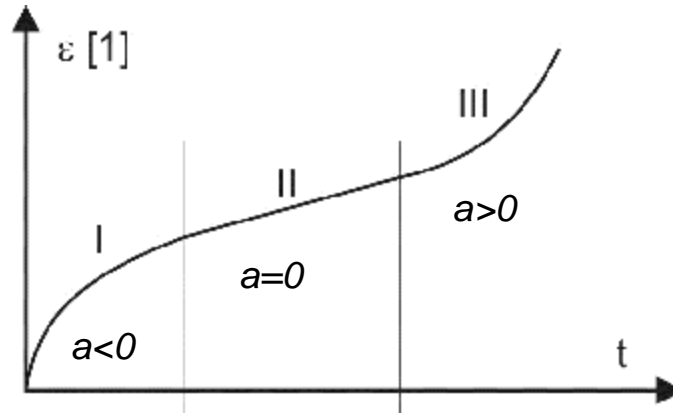
Stress path analysis of notch ligaments in the p-q diagram



Cohesions and friction angles of a burnt magnesia chromite material

S. Jin, D. Gruber, H. Harmuth, R. Roessler. Thermomechanical failure modeling and investigation into lining optimization for a Ruhrstahl Heraeus snorkel. Engineering Failure Analysis, 2016, 62: 254-262.

## Material constitutive model accounting for creep



Norton-Bailey strain hardening/softening creep formulation

$$\dot{\epsilon}_{cr} = K(T) \sigma^n \epsilon_{cr}^a$$

$K$ : a temperature function

$n$ : the stress exponent

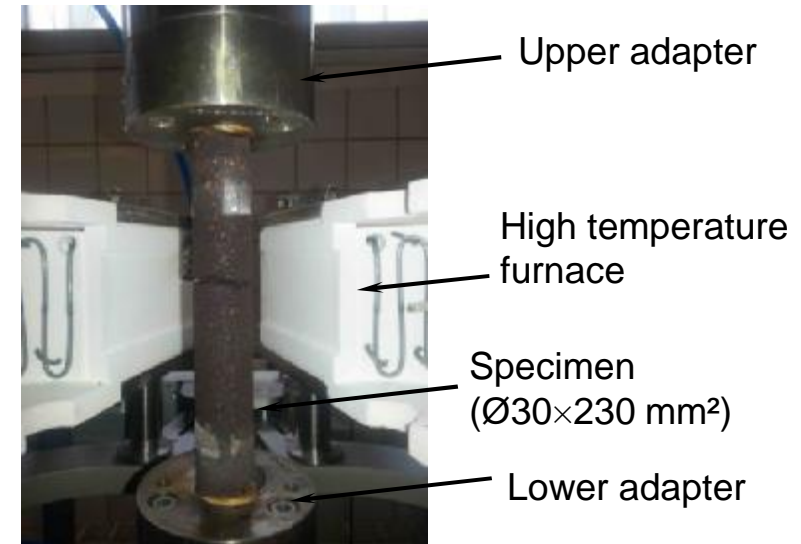
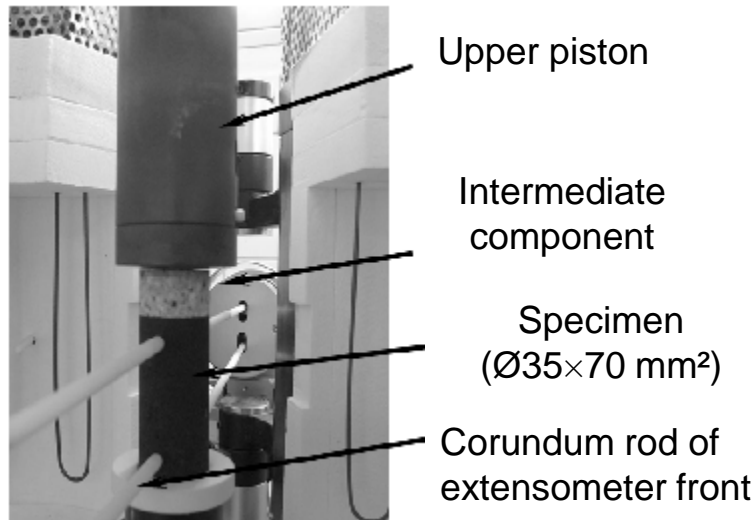
$a$ : the creep strain exponent

- I: primary stage
- II: secondary stage
- III: tertiary stage

Comments on creep in compression (CIC, European standard EN 993-9)

- 1) **Ambiguous onset** of creep due to a heating up under load (0.2MPa)
- 2) Rather **low load level** ( maximum load up to 0.2MPa) will not allow for the determination of Norton-Bailey creep rate equation in a wide load range
- 3) **Measurement of the displacement at the end faces of the specimen**

## Characterization method for creep



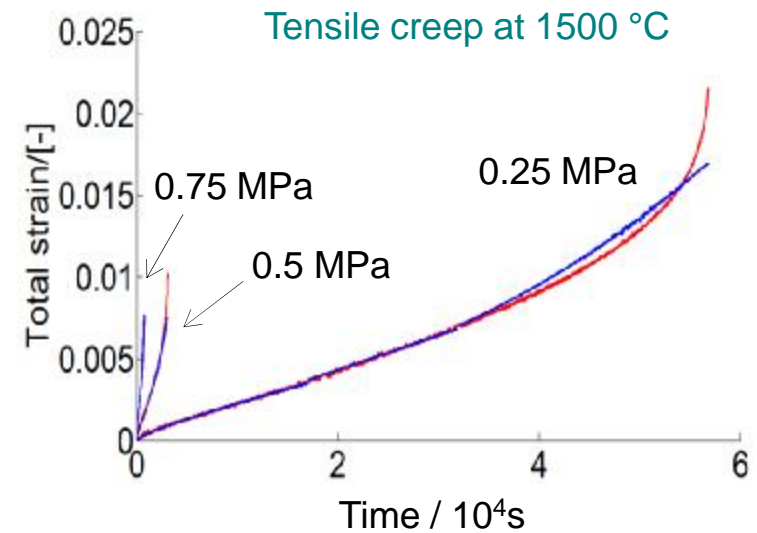
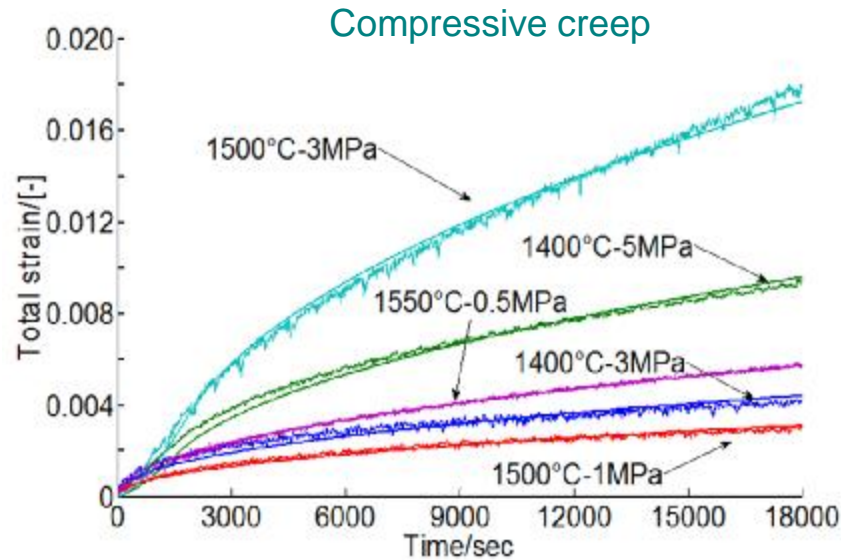
Setup of the high temperature creep measurements (left: compressive; right: tensile)

- Loads up to 20KN
- Uneven loading is avoided
- Deformation measurements on cylindrical surface of specimen with extensometers
- The height/diameter ratio of 2 allows the deformation measurements without influence from the end face friction in the case of compressive loading
- Creep origin is well defined

S. Jin, D. Gruber, H. Harmuth. Compressive creep testing of refractories at elevated loads-Device, material law and evaluation techniques. Journal of the European Ceramic Society, 2014, 34(15): 4037-4042.

Sidi Mammam A, Gruber D, Harmuth H, Jin S. Tensile creep measurements of refractories at service related loads including setup, creep law, testing and evaluation procedures. Ceramics International, 2016, 42(6) : 6791-6799.

## Characterization method for creep

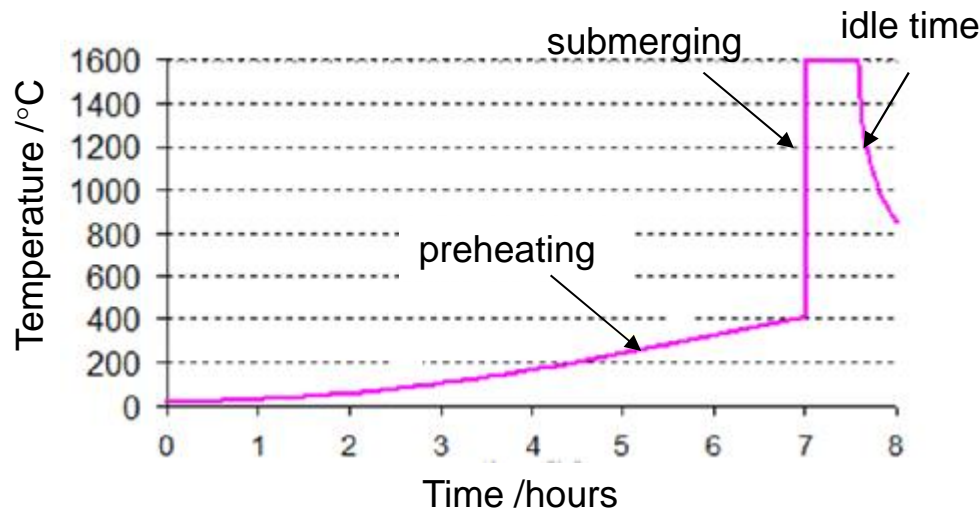
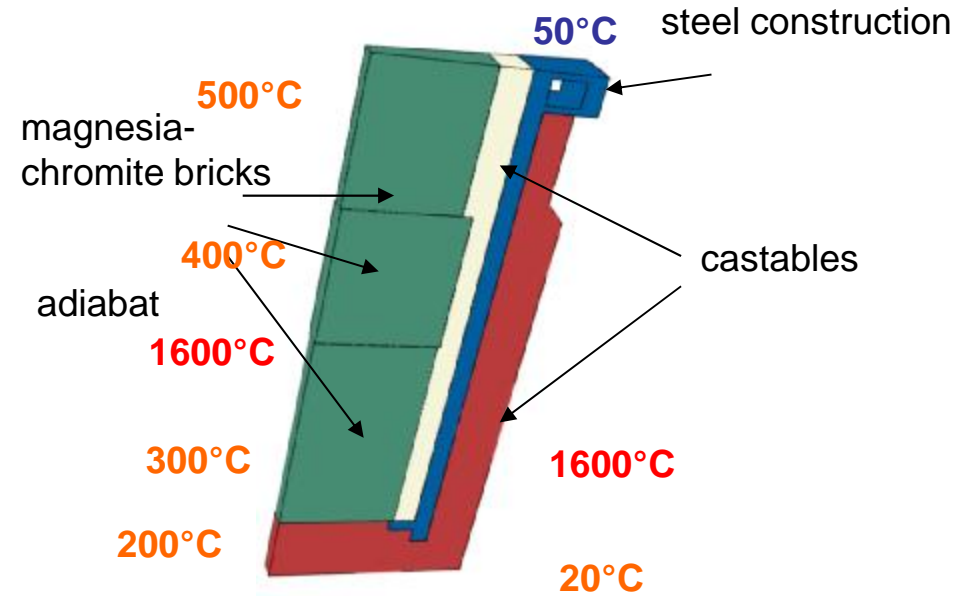


Primary creep parameters  $n$ ,  $a$  and  $K$  [ $\text{MPa}^{-n}\text{s}^{-1}$ ] of the magnesia chromite material at 1400 °C and 1500 °C in tension and compression

Loading		Temperature	1400 °C	1500 °C
		Tension	K	2.31E-07
a	- 0.15		- 0.22	
n	2.82		3.13	
Compression	K	1.24E-11	2.20E-10	
	a	-1.04	-1.04	
	n	3.20	3.20	



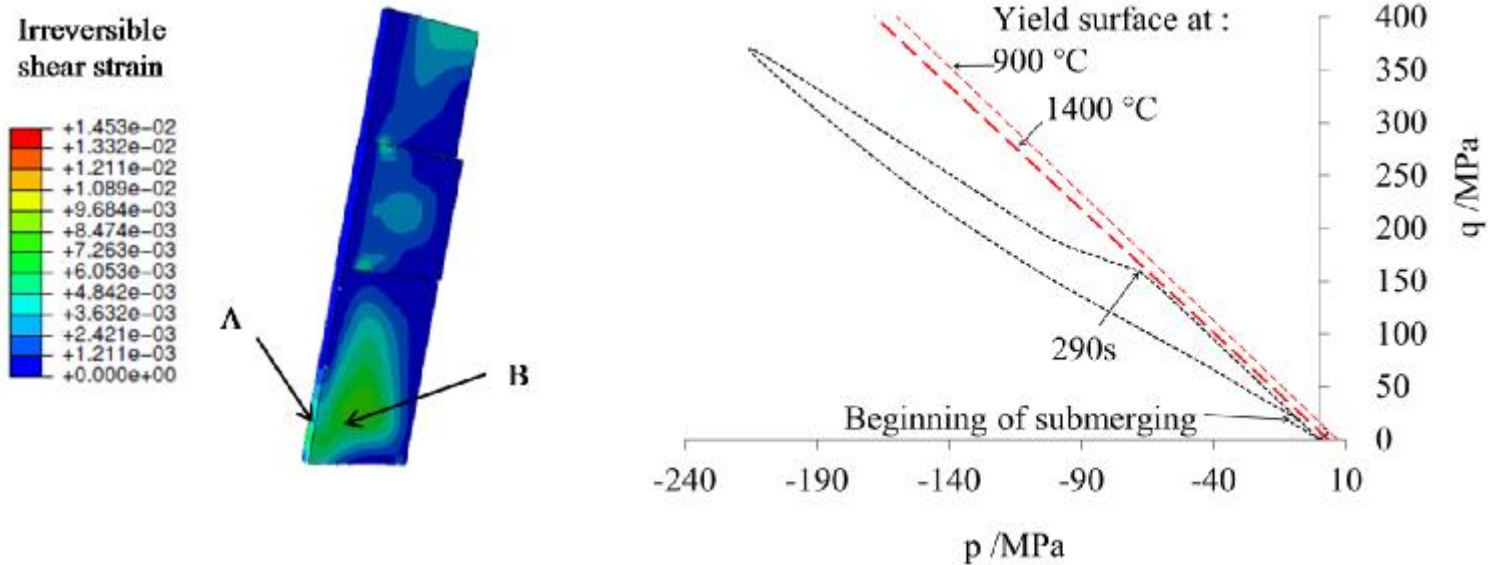
Ruhrstahl Heraeus (RH) snorkel



A process of a RH snorkel

- Shear failure and creep were considered for the magnesia chromite bricks in the working lining



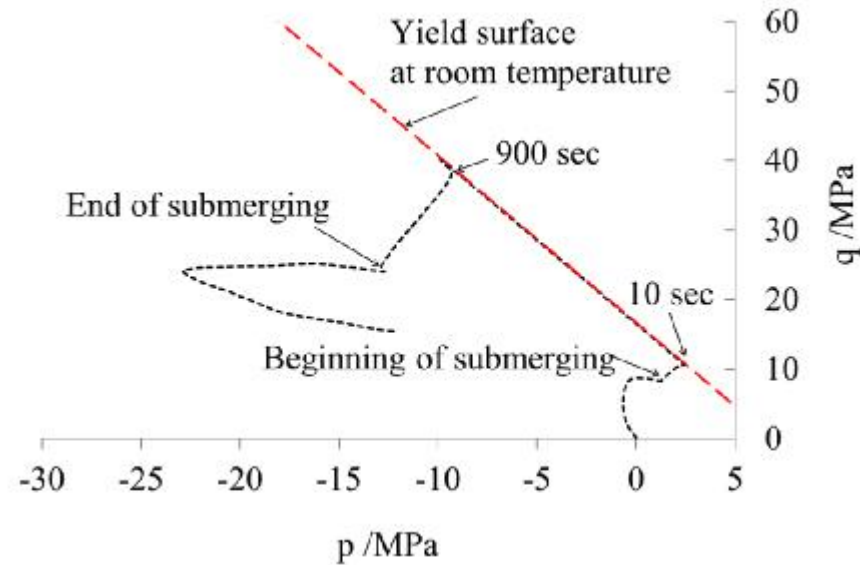
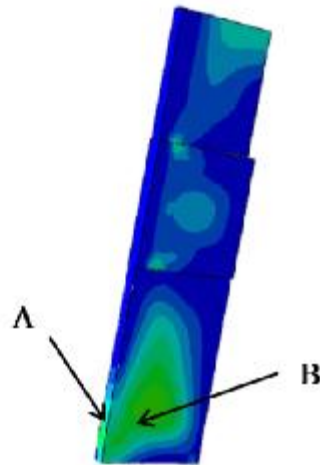
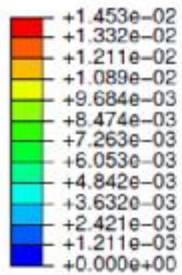


Stress path of point A in the p-q diagram

- The hot face experienced shear failure and creep after 290s submerging
- Tensile failure occurred during the idle time

S. Jin, D. Gruber, H. Harmuth, R. Roessler. Thermomechanical failure modeling and investigation into lining optimization for a Ruhrstahl Heraeus snorkel. Engineering Failure Analysis, 2016, 62: 254-262.

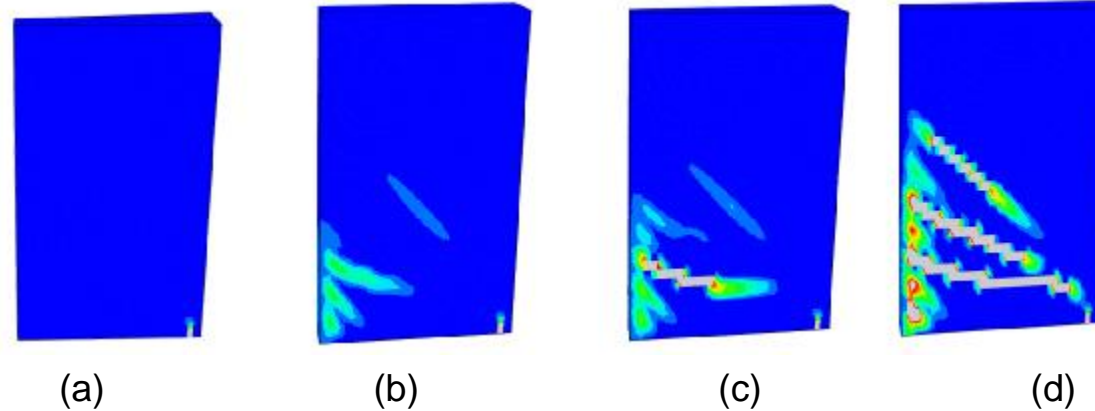
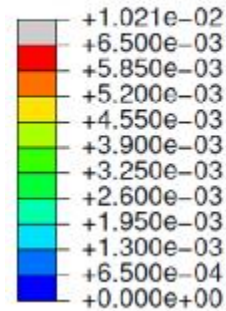
Irreversible shear strain



Stress path of point B in the p-q diagram

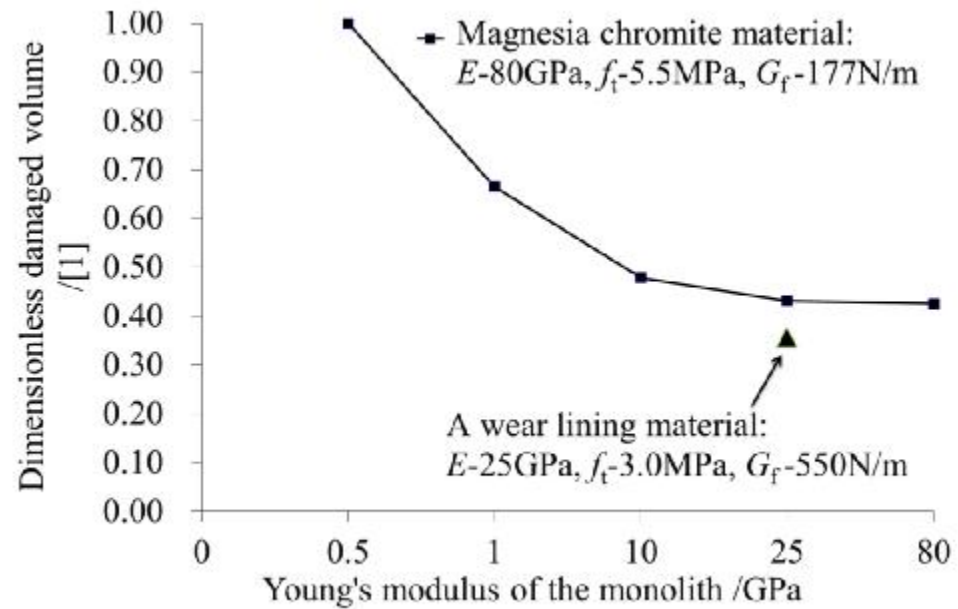
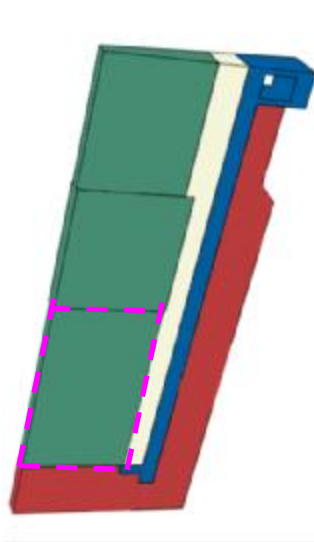
- The area close to the hot face experienced **tensile failure** at the beginning of submerging

S. Jin, D. Gruber, H. Harmuth, R. Roessler. Thermomechanical failure modeling and investigation into lining optimization for a Ruhrstahl Heraeus snorkel. Engineering Failure Analysis, 2016, 62: 254-262.

**Irreversible strain  
due to tension**


Distribution of irreversible equivalent tensile strains due to tension at the lowest section at a) the end of preheating, b) 1 s of submerging, c) 2 s of submerging, d) 7.6 s of submerging

- Fictitious crack model was applied to account for **tensile failure caused by thermal shock**
- **Cracks** occurred close to the hot face in 1s
- **Cracks propagated** inclined to the bottom of the lowest section



Dimensionless damaged volume of the lowest wear lining section based on various lining concepts

- Tensile failure were allowed in the monolith for the case study
- A well elaboration of lining concept can mitigate the damage volume with understanding of thermomechanical wear mechanisms

S. Jin, D. Gruber, H. Harmuth, R. Roessler. Thermomechanical failure modeling and investigation into lining optimization for a Ruhrstahl Heraeus snorkel. Engineering Failure Analysis, 2016, 62: 254-262.

- The **wedge splitting** test, modified **shear** test, and uniaxial **tensile** and **compressive creep** tests were applied for refractories;
- These advanced testing procedures provide **quantitative definitions** of refractory mechanical behavior at high temperatures;
- The understanding of **thermomechanical wear mechanisms of refractories** in service, and **lining optimization** were enhanced accordingly.

Vielen Dank für Ihre  
Aufmerksamkeit